Introduction

Technological developments in digital imaging highlight the need to optimize acquisition protocols. Radiographers need to understand thoroughly how the different acquisition options affect patient dose and image quality. The level of image quality should be adequate enough to provide diagnostic information at the lowest possible dose, without jeopardising diagnosis (1). Exposure optimization should protect patients from unnecessary dose and the ALARP (As Low As Reasonable Practicable) principle should always be kept in mind. Radiographers must constantly bear in mind this important principle because unfortunately digital radiology systems allow examinations to be performed over a wide range of exposure factors, and therefore patient doses. X-ray beam quality and quantity is dependent upon kVp and mAs. Improvement in image contrast and noise is seen when mAs increases; however such an increase could elevate patient dose unnecessarily. With digital technology 'overexposure' (using too high a dose than necessary) can occur whilst perceptual image quality remains acceptable (2). A result of this is the potential for dose creep to occur, with little or no diagnostic outcome benefit. However, if technology and acquisition protocols are managed adequately then dose reductions should occur without compromising image quality or diagnostic outcome.

Pelvis and hip radiography are consistently found to be amongst the highest contributors to effective dose (E) in all ten DOSE DATAMED countries in Europe, representing 2.8 to 9.4% of total collective dose (S) in the TOP 20 examinations list. The range of the percentage contribution to the total frequency from pelvis and hip examinations over the ten countries varies from 6.3 to 10% of total frequency, as reported by the European Commission (3). For pelvic imaging, changes within the clinical setting together with technological developments have seen a decline in patient dose (4). This is important because pelvic examinations involve exposing the gonads to ionising radiation.

When performing pelvis X-ray imaging the radiographer should modify X-ray exposure factors according to patient characteristics. This could involve altering kVp and/or mAs. Both of these alter dose to patient and image quality (5). Alongside this the radiographer could choose to use automatic exposure control (AEC) or manual mode (no AEC).

Increasing kVp by 10 whilst halving mAs is considered to offer similar perceptual image quality when compared with the original exposure factors; this approach is referred to as the 10 kVp rule (6,7). Importantly, application of the 10kVp rule in manual mode for anthropomorphic chest phantom imaging, across a wide range of exposure factors, provides consistent dose reductions (7). Allen *et al* (7) suggests further research should be conducted to determine whether the 10 kVp rule would have

value for a range of examinations using both CR and DR systems, especially in areas of low contrast like the pelvis.

In light of the 10 kVp rule, this study investigates the influence of kVp variation in relation to perceptual image quality and E for anthropomorphic phantom pelvis imaging using AEC and manual mode on a Computed Radiography (CR) system.

Methods and Materials

Our method was based upon previous studies in chest radiography (2,7). Perceptual image quality was evaluated using the two-alternative forced-choice (2AFC) method (8), with image quality criteria being derived from a psychometric scale (9). Effective dose was estimated using a Monte Carlo mathematical simulation.

A quantitative experiment was undertaken using a Rando® SK250 sectional lower torso anthropomorphic phantom (Figure 1). This pelvis phantom (10) simulates the x-ray absorbency, atomic number and specific gravity of soft human tissue. It includes the lumbar vertebrae, bony pelvis and the upper third of the femur. A hollow cavity reproduces the interior of the sigmoid flexure.

Figure 1. Anthropometric pelvis and upper third of femur with a hollow cavity to reproduce the sigmoid, diverticulum and rectum. Human bones are reconstructed to an average male size to simulate x-ray absorbency anatomical. The markings were used for accuracy in positioning

Image production

To determine the kVp and mAs impact using AEC and non-AEC / manual mode on image quality and E a series of X-ray images were produced; two experiments were conducted (one using AEC and one using manual mode). The images were acquired at 10kVp increments ranging from 60-120kVp for both experiments using the Wolverson Arcoma X-ray with a high frequency generator and a VARIAN 130 HS X-ray tube, with an inherent filtration of 3 mm Aluminium. An Agfa CR 35x43 image receptor (IR) was used for acquisition and processed in an Agfa CR 35-X digitiser with a spatial resolution of 10 pixel/mm and grey scale resolution of 12 bits per pixel. Images were produced with fixed source image distance (110 cm source-to-image-distance - SID), 35x43cm collimation, anti-scatter grid and broad focus spot (1 mm).

The first experiment produced 49 images based on seven AEC combinations using three chambers, producing a range of kVp and mAs values. From the lowest and highest produced mAs values obtained in the first experiment, the mean mAs from each kVp increment was used as a baseline for the second experiment (manual mode) which produced 35 images. These had increments and decrements calculated using percentiles of 25% to assess the 10 kVp rule influence on perceptual image quality and E in manual mode.

Perceptual image quality assessment and scoring

A total of 84 images were produced from both experiments. A panel of 5 experienced radiographers were invited to participate as observers to independently score the images using the 2AFC method. Bespoke 2AFC software was used to display the images and capture observer scores (11). When 2AFC is compared to other visual methods of image quality assessment, it is found to be easy and quick to complete and also offer more reliable responses than simple visual grading of single images (8). 2AFC involves presenting the observer with two images with one of the images being a reference image. The reference image was chosen by objectively measuring two bony regions of interest (ROI) on the left and right side of the pelvis to assess mean pixel values (Figure 2). The right region was calculated by the differences between ROI 1 and ROI 3 and the left region was calculated between ROI 2 and ROI 4. For the measurements, the iliac bone and the intertrochanteric region for both sides were considered. ImageJ software (12) was used to calculate the ROIs for every image and an average mean was obtained to select the reference image.

Figure 2. The ROI is shown in the form of a circle in the three regions in 'image J' and calculated for calcium densities. The contrast was calculated by the differences between two ROI .i.e. 1 and 3. This image shows the ROI for the reference image.

The reference image was chosen based on the mean pixel value difference from ROIs, from an intermediate value of the highest and the lowest pixel difference obtained in the right and left regions of all 84 images. The identified reference image (#34) was obtained from an exposure using all AEC chambers, at 90 kVp and 11.2 mAs and an E of 0.104mSv.

Images were displayed on two 24.1 inch NEC (EA243WM) monitors with a resolution of 2.3 megapixels resolution calibrated to DICOM GSDF (luminance of >170 cd/m2) and a low level lighting was used in the viewing area (13).

Anatomical areas and noise perception for each image were compared against the reference image. Table 1 indicates the anatomical areas and the statements used for comparison using 2AFC. The items were derived from a psychometric scale which was under development at the time of this research (9). Image quality scoring criteria, indicated in Table 1, was based on a 5 Likert point scale, where: (1) much worse than; (2) slightly worse than; (3) equal to; (4) better than; (5) much better than, the reference image.

Table 1. Image quality scoring criteria

Effective dose (E) estimation

Monte Carlo simulation software (PCXMC) was used to estimate E from the dose area product (DAP) and the acquisition parameters. Effective dose data were analysed in the two experiments to statistically describe the effect of independent variables such as kVp and mAs at the different kVp settings.

2AFC and E were transferred to SPSS software (version 21.0) for statistical analysis. One-way between groups analysis of variance (ANOVA) at a 5% level was conducted to test for any significant difference between tube potentials concerning image quality scores and E.

Results

Perceptual image quality

The maximum image quality score (%) obtained from all the observers at 10 kVp increments and incorporating all mAs values for AEC and manual mode images is shown in table 2.

Table 2. Maximum image quality global score (%) from all observers at 10 kVp increments for all mAs values

In manual mode exposures, the maximum score varies from 94% at 60 kVp to 80% in all tube potential settings ranging from 90 kVp to 120 kVp. Although a decrease in image quality as the kVp increases is observed, image quality is maintained at 80% of higher kVp options. The highest value in AEC exposures is obtained at 60 kVp (100%); using the left chamber, however, the score is almost

halved at 120 kVp (56%). While increasing kVp at 10 kVp increases in all possible AEC combinations, the observed trend is a decrease in the maximum image quality score, where 54% is achieved at 120 kVp using the central chamber.

Table 3 demonstrates the average image quality global score (%) and standard deviation (sd) from all observers at 10 kVp increments for all mAs values.

Table 3. Average image quality global score (%) and standard deviation (sd) from all observers at 10 kVp increments for all mAs values

For the manual mode a decrease in image quality is observed while tube potential increases from 73.9% (sd 8.8) at 60 kVp to 49.0% (sd 1.3) at 120 kVp. For the AEC exposures the same trend is observed with the left chamber having a better performance in general when compared to other options reflecting a steady decrease in the average image quality from 77.2% (sd 17.8) at 60 kVp to 48.0% (sd 6.3) at 120 kVp.

Figure 3. Image quality mean and Confidence Interval (95% CI) from all observers at 10 kVp increments for all mAs values

Figure 3 represents the mean, maximum and minimum changes in image quality scores, (95% Confidence Interval - CI) at each kVp value. The mean image quality values scored above the reference image (RI represented by the horizontal line) suggests improved image quality; whereas values below the RI indicate a decrease in image quality. The mean perceptual decrease in image quality occurs at higher tube potential settings (>90 kVp).

Manual mode images demonstrate strongest CI, whereas the CI is lower in images produced by the left chamber. Also a stronger CI in image scoring is demonstrated at kVp >90. The CI between left and right regions of the pelvis demonstrates a similar perceptual value throughout the mean image scoring.

The results show that the mean values for noise, derived from 2AFC scoring, range from 2.8 to 3.2. This suggests that the visual appreciation of noise is very similar and with little variation from the reference image, indicating that the images were assessed as “equal to” the reference image.

Effective dose (E)

In figure 4 a box and whiskers plot shows the variation of E for each kVp increment incorporating all mAs values for manual mode images.

Figure 4. Effective dose (mSv) boxplot at 10 kVp increments for all mAs values

The median (50th percentile) of E is represented by the line in the center of the box, while the upper quartile represents the 75th percentile above the median, whereas the lower quartile signifies the 25th percentile below the median. The maximum and minimum points (whiskers) demonstrate E at extreme values for each kVp. The results show a decrease in the 75th quartile E from 0.37 mSv at 60 kVp to 0.13 mSv at 120kVp. A decrease is also observed in all AEC combinations from 60 kVp to 120 kVp. The higher E at 60 kVp is found while using the right chamber (0.30 mSv) and the lower E using the left (center combination (0.22 mSv). At 120 kVp the values are substantially lower ranging from 0.08 mSv (right chamber) to 0.07 mSv (central chamber). Figure 4 illustrates that when the 10 kVp rule is applied E decreases.

A One-Way ANOVA was performed to test for significant differences between kVp values concerning image quality scores and E. In regard of image quality scores, no statistically significant differences were observed in manual mode and in five possible AEC combinations ($p \geq 0.05$), except in two AEC combinations: when using all AEC chambers and also when using only the left chamber. Concerning E, statistically significant differences ($p=0.000$) were observed at all tube potential variation in manual mode and in three AEC mode combinations: left; centre; and left/centre.

Discussion

A decrease in perceptual image quality as the kVp increases was observed both in manual mode and AEC experiments, however no significant statistical differences ($p>0.05$) were found except in two chamber combinations. Image quality scores at 10 kVp increments for all mAs values using manual mode demonstrates a better score up to 90kVp.

The 10 kVp rule is generally well tolerated in pelvis radiographs concerning the perceptual image quality compared to the reference image, according to the results achieved up to 90 kVp. This is reflected visually in figure 3 and tables 2 and 3. The 10 kVp rule has a tendency to breakdown for image quality at higher kVp values (ie 100-120 kVp). This trend appears to be opposite to research conducted in the chest (7) - where higher kVp and lower mAs seems to have a better effect on image quality, perhaps due to composition of this body part.

The results demonstrate differences using the AEC and manual mode combinations when varying the kVp. Tables 2 and 3 show the best image quality corresponds to the lowest kVp value (60kVp) with the left chamber. Maximum image quality global score ranges are similar at 60kVp and 120kVp as data identifies the same perceptual differences. Average image global quality score standard deviation shows an increase in Manuela mode combinations in table 2 as a result of differing exposure factors in this group.

Figure 3 shows that manual mode and AEC combinations have a decrease in image quality after 90kVp. A stronger confidence interval is demonstrated after 90kVp due to the reduction in mean pixel value at high kVp's.

E results show a statistically significant decrease (p=0.000) on the 75th percentile from 0.37 mSv at 60 kVp to 0.13 mSv at 120kVp when applying the 10 kVp rule in manual mode. Although no relationship between image quality and E was tested in this study, maximum image quality global score ranges are similar at 60kVp and 120kVp as data identifies the same perceptual differences while a marked reduction in E is observed when applying the 10 kVp rule.

The study has some limitations, one of which was the inability to select 50% reduction of mAs values from the Wolverson Arcoma X-ray unit control panel, as occurred in Allen's study (7). Instances where desired mAs could not be achieved, the nearest mAs figure were selected. For example, when 24mAs was required, only 23 and 26mAs could be selected. Therefore, the nearest value of 23 mAs was chosen.

The data was acquired using Agfa CR system. Hence, it cannot be used to generalize to other manufacturers. Therefore, investigations should be performed using equipment from different manufacturers and also different technologies such as DR (digital radiology) systems.

Conclusion

For AEC and manual acquisition modes image quality, assessed by 2AFC, remains similar before and after the 10kVp rule has been applied, albeit above 90kVp there is a tendency for the quality to reduce. E decreases as kVp increases. The 10kVp rule shows promise in pelvis imaging for AEC and manual mode acquisition modes.

References

1. Martin CJ. Management of patient dose in radiology in the UK. Radiat. Prot. Dosimetry [Internet]. 2011 Nov [cited 2012 Mar 26];147(3):355–72. Available from: http://www.ncbi.nlm.nih.gov/pubmed/22008582

2. Ma WK, Hogg P, Tootell a., Manning D, Thomas N, Kane T, et al. Anthropomorphic chest phantom imaging – The potential for dose creep in computed radiography. Radiography

[Internet]. 2013 Aug [cited 2013 Nov 18];19(3):207–11. Available from: http://linkinghub.elsevier.com/retrieve/pii/S1078817413000424

3. European Commission. Radiation Protection N° 154 European Guidance on Estimating Population Doses from Medical X-Ray Procedures [Internet]. 2008. Available from: http://ddmed.eu/_media/background_of_ddm1:rp154.pdf

4. Ofori EK, Antwi WK, Scutt DN, Ward M. Optimization of patient radiation protection in pelvic X-ray examination in Ghana. J. Appl. Clin. Med. Phys. [Internet]. 2012 Jan;13(4):3719. Available from: http://www.ncbi.nlm.nih.gov/pubmed/22766943

5. Lança L, Silva A. Technical Considerations Concerning Digital Technologies. Digit. Imaging Syst. Plain Radiogr. New York: Springer; 2013. p. 37–47.

6. Brennan PC, McCandless N, Masterson J. Modern day film-screen combinations do not obey conventional exposure rules. Radiography [Internet]. 1997;3(4):305–10. Available from: http://www.scopus.com/inward/record.url?eid=2-s2.0-0030723703&partnerID=40&md5=1ba8e96402a7342a3f8b01918945a2cd

7. Allen E, Hogg P, Ma WK, Szczepura K. Fact or fiction: An analysis of the 10 kVp “rule” in computed radiography. Radiography [Internet]. 2013 Aug [cited 2013 Nov 16];19(3):223–7. Available from: http://linkinghub.elsevier.com/retrieve/pii/S1078817413000497

8. Burgess AE. Visual perception studies and observer models in medical imaging. Semin. Nucl. Med. [Internet]. Elsevier Inc.; 2011 Nov [cited 2013 Nov 18];41(6):419–36. Available from: http://www.ncbi.nlm.nih.gov/pubmed/21978445

9. Mraity H, Hogg P. Development and Validation of a Psychometric Scale for Assessing Pelvis Image Quality. University of Salford; 2013.

10. The Phantom Laboratory. Sectional Lower Torso SK250 [Internet]. 2013 [cited 1BC Aug 27]. Available from: http://www.phantomlab.com/library/pdf/sectional_SK250DS.pdf

11. Hogg P, Blindell P. Software for image quality evaluation using a forced choice method. Manchester: United Kingdom Radiological Congress; 2012. p. 139.

12. Abràmoff MD, Hospitals I, Magalhães PJ, Abràmoff M. Image Processing with ImageJ [Internet]. 2004. Available from: http://rsbweb.nih.gov/ij/docs/faqs.html

13. Samei E, Badano A, Chakraborty D, Compton K, Cornelius C, Corrigan K, et al. Assessment of display performance for medical imaging systems: Executive summary of AAPM TG18 report. Med. Phys. [Internet]. 2005 [cited 2013 Nov 21];32(4):1205. Available from: http://link.aip.org/link/MPHYA6/v32/i4/p1205/s1&Agg=doi

Figure 1. Anthropometric pelvis and upper third of femur with a hollow cavity to reproduce the sigmoid, diverticulum and rectum. Human bones are reconstructed to an average male size to simulate x-ray absorbency anatomical. The markings were used for accuracy in positioning

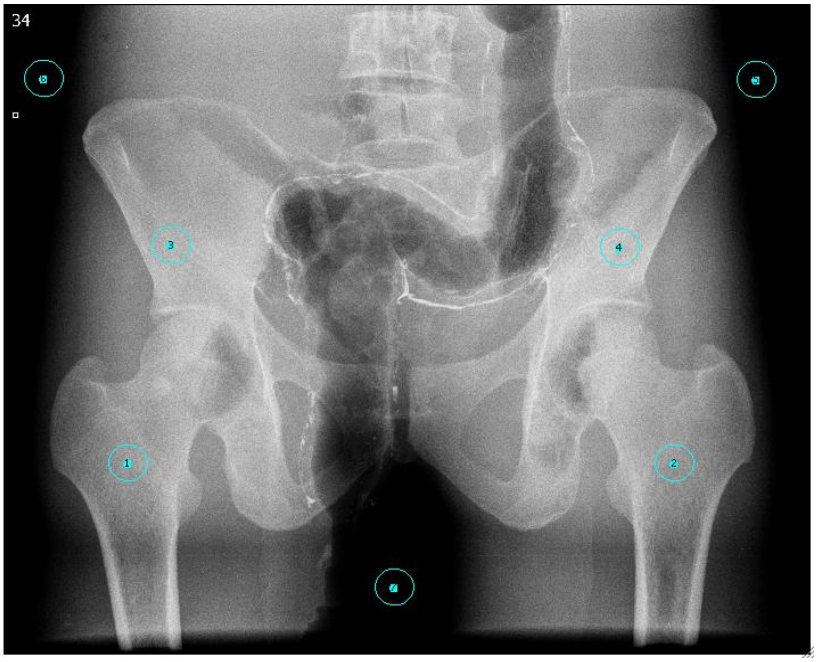

Figure 2. The ROI is shown in the form of a circle in the three regions in 'image J' and calculated for calcium densities. The contrast was calculated by the differences between two ROI .i.e. 1 and 3. This image shows the ROI for the reference image.

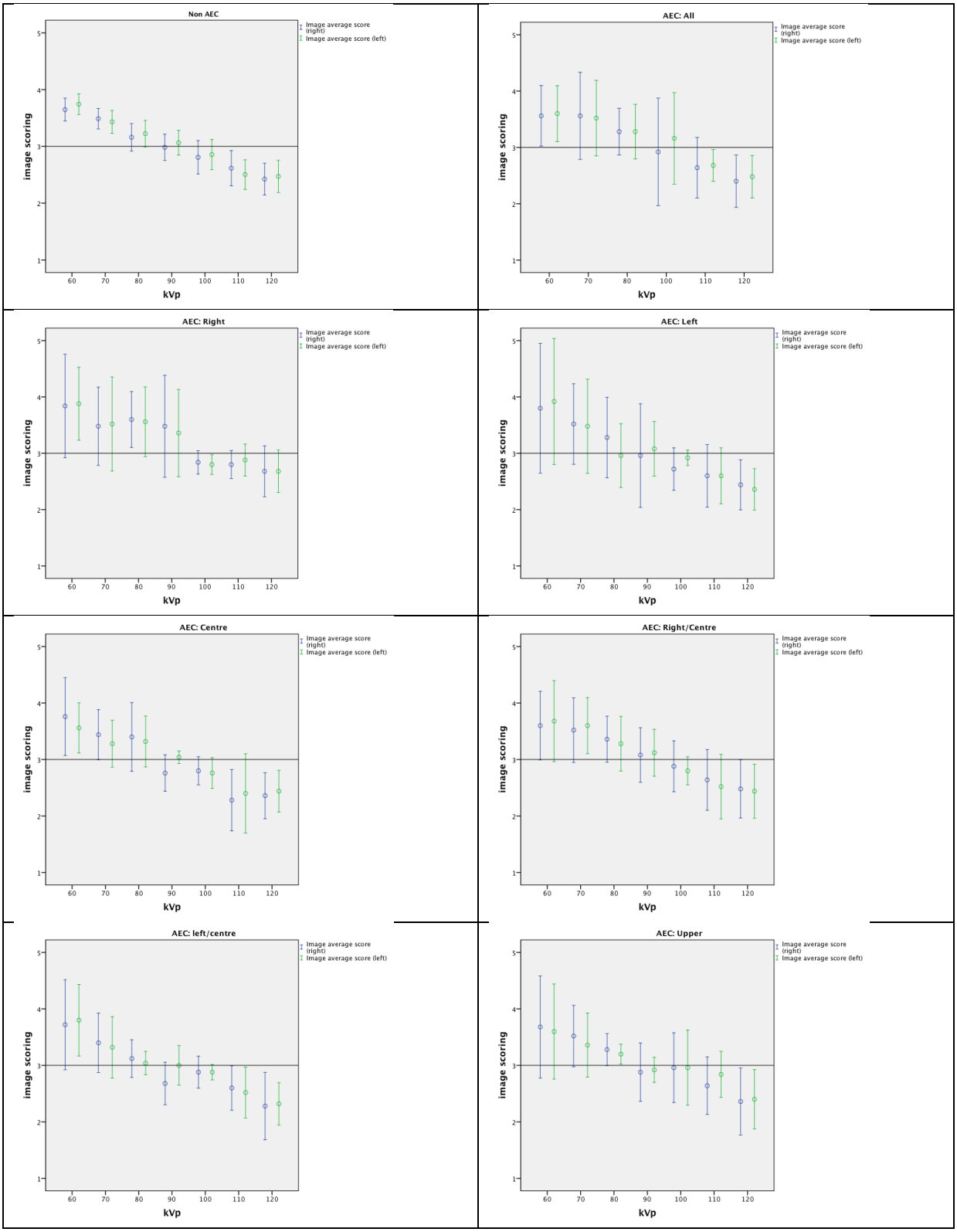

Figure 3. Image quality mean and Confidence Interval (95% CI) from all observers at 10 kVp increments for all mAs values

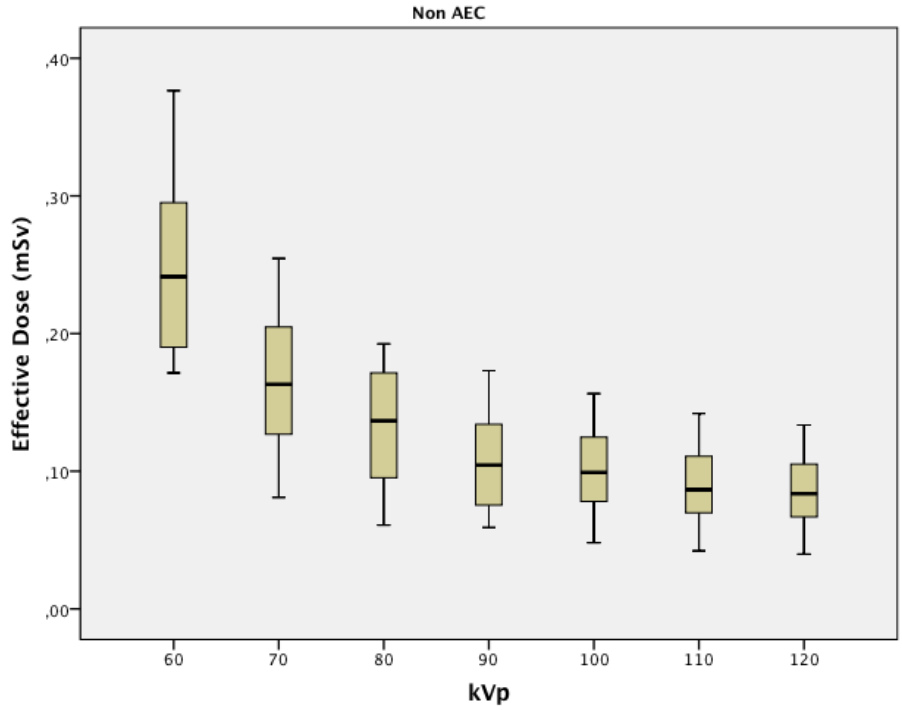

Figure 4. Effective dose (mSv) boxplot at 10 kVp increments for all mAs values

Table 1. Image quality scoring criteria

	Categories	Item #
Anatomic region	Right hip 5 items	2. The right lesser trochanter is visualised adequately 3. The right hip joint is adequately visualised 5. The right iliac crest is visualised adequately 6. The right greater trochanter is visualised adequately 11. The right femoral neck is visualized adequately
	Left hip 5 items	1. The left hip joint is adequately visualized 4 The left greater trochanter is visualised adequately 7. The left iliac crest is visualised adequately 8. The left lesser trochanter is visualised adequately 9. The left femoral neck is visualised adequately
Noise	Noise perception 1 item	10. There is a significant amount of noise in this image

Table 2. Maximum image quality global score (%) from all observers at 10 kVp increments for all mAs values

			kVp						
			60	70	80	90	100	110	120
Max image quality global score %	Non AEC		94	84	92	80	80	80	80
	AEC	All	78	84	76	R	80	58	60
		Right	96	82	80	80	60	60	60
		Left	100	84	76	76	60	62	56
		Centre	80	78	80	60	60	60	54
		Right/ Centre	82	78	74	68	62	62	60
		Left/c entre	90	80	66	60	60	60	56
		Upper	90	78	68	62	76	62	60

R= reference image

Table 3. Average image quality global score (%) and standard deviation (sd) from all observers at 10 kVp increments for all mAs values

			kVp						
			60	70	80	90	100	110	120
Average image quality global score % (sd)	Non AEC		73,9 (8,8)	69,2 (8,9)	63,8 (11,3)	60,5 (10,3)	56,6 (13,4)	51,2 (13,6)	49,0 (13,3)
	AEC	All	71,6 (7,9)	70,8 (11,4)	65,6 (7,1)	R	60,8 (14,2)	53,2 (4,6)	48,8 (6,4)
		Right	77,2 (12,5)	70,0 (12,2)	71,6 (8,9)	68,4 (13,2)	56,4 (2,6)	56,8 (3,0)	53,6 (6,2)
		Left	77,2 (17,8)	70,0 (11,7)	62,4 (9,9)	60,4 (10,6)	56,4 (3,3)	50,2 (8,0)	48,0 (6,3)
		Centre	73,2 (8,4)	67,2 (6,9)	67,2 (7,6)	58 (2,0)	55,6 (3,8)	46,8 (9,7)	48,0 (5,8)
		Right/ Centre	72,8 (10,5)	71,2 (8,3)	66,4 (6,5)	62 (7,1)	56,8 (4,6)	51,6 (8,6)	49,2 (7,4)
		Left/c entre	75,2 (11,4)	67,2 (8,4)	61,6 (4,3)	56,8 (5,0)	57,6 (1,7)	51,2 (6,7)	46,0 (7,6)
		Upper	72,8 (14,0)	68,8 (8,9)	64,8 (2,3)	58 (5,8)	59,2 (10,3)	54,8 (6,4)	47,6 (8,9)

R= reference image